Water-wave scattering by thick vertical barriers

MRIDULA KANORIA, D. P. DOLAI and B. N. MANDAL
Physics and Applied Mathematics Unit, Indian Statistical Institute, 203, B. T. Road, Calcutta – 700 035, India
e-mail: biren@www.isical.ac.in

Received 26 March 1997; accepted in revised form 9 October 1998

Abstract. This paper is concerned with two-dimensional scattering of a normally incident surface wave train on an obstacle in the form of a thick vertical barrier of rectangular cross section in water of uniform finite depth. Four different geometrical configurations of the barrier are considered. The barrier may be surface-piercing and partially immersed, or bottom-standing and submerged, or in the form of a submerged rectangular block not extending down to the bottom, or in the form of a thick vertical wall with a submerged gap. Appropriate multi-term Galerkin approximations involving ultraspherical Gegenbauer polynomials are used for solving the integral equations arising in the mathematical analysis. Very accurate numerical estimates for the reflection coefficient for each configuration of the barrier are then obtained. The reflection coefficient is depicted graphically against the wave number for each configuration. It is observed that the reflection coefficient depends significantly on the thickness for a wide range of values of the wave number, and as such, thickness plays a significant role in the modelling of efficient breakwaters.

Key words: water-wave scattering, thick barrier, multi-term Galerkin approximation, reflection coefficient.

1. Introduction

Breakwaters are constructed to protect a sheltered area by reflecting back the incident waves into the rough sea. The problems of water wave scattering by breakwaters modelled as thin vertical barriers of various configurations have been studied extensively in the literature under the assumption of linear theory during the last fifty years. The four basic configurations such as a surface-piercing partially immersed barrier, a submerged bottom-standing barrier, a submerged plate of finite vertical height and a wall with submerged gap or gaps have been used as basic models of breakwaters in the literature because of their simplicity in the engineering design and most importantly due to the ability to solve the associated water wave scattering problems expicitly for normally incident surface water waves in infinitely deep water. For these problems the velocity potential describing the resulting fluid motion can be obtained in closed form and the physical quantities of interest, such as the reflection and transmission coefficients, can also be obtained in terms of known functions or definite integrals (see *e.g.* [1–8]). A variety of mathematical techniques have been used to obtain the explicit solutions to these problems. The reason for the existence of explicit solutions is the fact that each of these problems is equivalent to solving the two-dimensional Laplace equation in a half plane with the condition of zero normal derivative of the function being sought for and the mixed condition on the free surface. By the use of complex variable theory, each problem can be reduced to finding a complex function satisfying certain conditions and having certain singularities, and this is somewhat straightforward in principle to obtain (see [9]). For obliquely incident waves, the complex-variable theory is not applicable and as such the explicit solutions to these problems are perhaps no longer possible to obtain. The same conclusion also applies

if the water is of uniform finite depth, while the waves are incident normally or obliquely on a barrier. In these cases, the associated water-wave scattering problems must be tackled mathematically by some approximate methods in order to obtain numerical estimates for the reflection and transmission coefficients.

For obliquely incident waves on a surface-piercing thin vertical barrier partially immersed in deep water, Evans and Morris [10] obtainined good complementary bounds for the reflection coefficient by using single-term Galerkin approximations for solving two integral equations, one for the horizontal velocity across the gap below the barrier and the other for the difference of velocity potential across the barrier. The single-term approximations are chosen in terms of the explicit results of Ursell [1]. The bounds involve some definite integrals, and when computed numerically, coincide up to one or two decimal places, and as such their averages produce fairly good numerical estimates for the reflection coefficient. Again, for oblique incidence on a thin vertical plate or a wall with a gap submerged in deep water Mandal and Das [11] and Das [12] *et al*. used this technique successfully to obtain fairly good estimates for the reflection coefficient in each case. In fact, any water-wave scattering problem involving a thin vertical barrier with gaps above or below or in between, in deep or uniform finite depth water, can be tackled by this technique in principle, wherein the single-term approximations involve the corresponding exact solutions for normal incidence and deep water. However, there is no guarantee that the technique would result in good complementary bounds for any scattering problem involving a vertical barrier. For example, when surface waves are obliquely incident on a thin vertical barrier submerged in deep water, Evans and Morris [10] reported that the bounds are not very close and as such the single-term approximation technique is not suitable for this case.

In water of uniform finite depth, Losada [13] *et al.* investigated two oblique wave scattering problems involving a thin vertical barrier with gaps by a method in which each problem is reduced to finding the solution of a dual series relation. Using the principle of least squares, they reduced the dual-series relation to an infinite linear system which was then solved numerically after truncation, and this solution was utilized to obtain the reflection and transmission coefficients numerically. The case of normal incidence could be tackled by the same method. Later Mandal and Dolai [14] utilized the single-term Galerkin approximation technique involving the corresponding known exact solutions for normally incident waves in deep water to obtain very accurate bounds for the reflection coefficients for four water-wave scattering problems involving thin vertical barriers with gaps in finite depth water.

Several scattering problems involving two symmetrical thin vertical barriers with gaps have also been tackled by the single-term Galerkin approximation technique. By virtue the geometrical symmetry, each problem was replaced by two separate problems, each involving a single barrier, which was then tackled by this technique. For the case of infinitely deep water, Evans and Morris [15] earlier used this technique to handle the problem of water-wave scattering by two thin vertical parallel barriers immersed to a given depth below the free surface. Recently, Kanoria and Mandal [16], Banerjea [17] *et al.* investigated a number of oblique wave-scattering problems involving two symmetrical thin vertical barriers with gaps in uniform finite depth water by using this technique. It may be noted that the numerical estimates for the reflection coefficients in each of these problems are accurate mostly up to one or two decimal places depending on the wave number of the incident wave field and the geometry of the barriers.

As mentioned earlier, the single-term Galerkin approximation technique does not always lead to even moderately accurate bounds for the reflection coefficients in a number of wave-

scattering problems involving thin vertical barriers either in deep water or in water of uniform finite depth. Thus, the technique needs to be modified. An obvious modification is perhaps the use of multi-term Galerkin approximations. For single-term approximations, the exact solutions for deep water and normal incidence of the waves involving the barrier have been utilized. However, for multi-term approximations, we need to find appropriate basis functions in terms of which multi-term expansions can be made. Although, in principle, any set of independent functions would serve the purpose, in practice, the basis functions are to be chosen suitably such that very accurate numerical estimates for the reflection and transmission coefficients are obtained with minimum effort. For a number of scattering problems involving thin vertical barriers, Porter and Evans [9] showed how appropriate basis functions in terms of Chebyshev polynomials can be chosen to produce extremely accurate numerical results with minimum effort. Banerjea [17] *et al.* and Das [18] *et al.* utilized the multi-term Galerkin approximation technique successfully for a number of water-wave scattering problems involving two symmetric thin vertical barriers with gaps in finite-depth water.

For a thin wall with a submerged *narrow* gap, the method of matched asymptotic expansion has been utilized with great success to study the related water wave scattering problems. Tuck [19] first used this method to obtain an approximate expression for the transmission coefficient when a surface wave train is normally incident on a thin vertical wall with a *narrow* gap submerged in deep water. Although the explicit solution to this problem, when the gap is not necessarily narrow, was obtained by Porter [7] shortly afterwards, Tuck [20] later mentioned the usefulness of the approximate result for the transmission coefficient for a narrow gap over Porter's [7] result which is limited to sharp edged gaps in plane walls of zero thickness. Packham and Williams [21] generalised Tuck's [19] narrow-gap problem in deep water to water of uniform finite depth and used an integral-equation formulation based on application of Green's integral theorem in the fluid region to tackle the problem. They solved the integral equation approximately by exploiting the concept of narrowness of the gap and used this solution to obtain an expression of the transmission coefficeint, which reduces to Tuck's [19] result as the depth of water is made to tend to infinity. Also, Mandal [22] reinvestigated Tuck's [19] narrow-gap problem by using an integral-equation formulation based on Havelock's [23] expansion of water-wave potential. These authors solved the integral equation approximately by using the method of Packham and Williams [21] and then Tuck's [19] approximate expression for the transmission coefficient was derived.

Guiney [24] *et al.* extended the work of Tuck [19] to include the effect of thickness in a vertical wall of rectangular cross section while Owen and Bhatt [25] considered the case of a narrow gap in a thick barrier of arbitrary cross section. Tuck [20] also discussed the role of matched-asymptotic-expansion technique in some detail in tackling problems of flow through small holes in an expository article. Liu and Wu ([26], [27]) used Tuck's [19] method of matched asymptotic expansions to investigate oblique wave scattering by a thick wall with a submerged narrow gap in finite-depth water and also in deep water. However, their investigation was actually limited to the long-wave case only, since they approximated the modified Helmholtz equation in two dimensions by the Laplace equation for obtaining the *inner* solution. It may be noted that the method of matched asymptotic expansions is not suitable for narrow gaps.

When the breakwaters are modelled as thick vertical barriers with rectangular cross sections in water of uniform finite depth, the corresponding water-wave scattering problems for normal incidence of a surface wave train were investigated by Mei and Black [28] for surface-piercing and bottom-standing barriers. They used a variational formulation to obtain numerical

estimates for the reflection coefficient with an accuracy within one percent and presented graphically the numerical results.

In this paper we consider two-dimensional scattering of a train of surface water waves normally incident on a thick vertical barrier of rectangular cross section in water of uniform finite depth. The barrier has four different geometrical configurations designated by type I, type II, type III and type IV depending on whether it is surface piercing and partially immersed, bottom standing and submerged, in the form of a submerged rectangular block not extending down to the bottom, or in the form of a thick vertical wall with a submerged gap. In the latter configuration, the gap is not necessarily narrow. By use of the geometrical symmetry of a barrier about its center line, the scattering problem for each type of barriers is split into two separate problems involving the symmetric and anti-symmetric potential functions describing the resulting motion in the fluid. Appropriate eigenfunction expansions for each of these potential functions in different regions followed by a matching process produce an integral equation for the corresponding unknown horizontal component of velocity across the vertical line through the corner points in the gap or gaps above or below the barrier. Also, for each case of the symmetric and antisymmetric potential functions, a real quantity related to the reflection coefficient is defined. This is expressed in terms of an integral expression involving the aforesaid unknown velocity. Thus, once the integral equations are solved, the reflection coefficient can be obtained. The two integral equations for each configuration of the barrier are solved here by suitable multi-term Galerkin approximations involving ultraspherical Gegenbauer polynomials. This idea of multi-term approximation involving Gegenbauer polynomials is due to Porter (*cf.* Evans and Fernyhough [29]) in connection with the mathematical study of a water wave problem concerning edge waves travelling along a periodic coast line consisting of a straight and vertical cliff face from which protrudes an infinite number of rectangular barriers.

We obtain the numerical results for the reflection coefficient for each thick-barrier configuration with a six-figure accuracy by choosing only four terms in the multi-term Galerkin approximations, and these are also depicted graphically against the wave number. For type I barriers, the resutls are compared with Mei and Black's [28] results and good agreement is achieved. For type II barriers, zeros of the reflection coefficient occur for a number of values of the wave number. This is consistent with the observations of Mei and Black [28]. For large horizontal length of type II barriers, the number of zeros of the reflection coefficient as a function of the wave number increases, which is also consistent with the observation of Newman [30] for long bottom obstacles. The results for type III barriers reduce to those for type II barriers if we take the lower end very near to the bottom, while the results for type IV barriers reduce to these for type I barriers if we make the height of the lower part very small. These results provide some checks on the correctness of the numerical method utilized here. Also, the results for type IV barriers are compared with narrow gap results of Packman and Williams [21] for thin barriers. Agreement in the qualitative behaviour of the reflection coefficient as a function of the wave number is seen to have been achieved.

2. Formulation of the problem

We consider a thick barrier of width $2b$ present in water of uniform finite depth h, and choose the y-axis vertically downwards along the line of symmetry of the thick barrier so that the wetted part of the barrier occupies the region $-b \leqslant x \leqslant b, y \in L = L_j\,(j = 1, 2, 3, 4)$.

Here $L_1 = (0, a)$, $L_2 = (c, h)$, $L_3 = (a, c)$ and $L_4 = (0, a) + (c, h)$ $(0 < a < c < h)$ corresponding to type I, type II and type III and type IV barrier configurations respectively. These configurations are described in Figure 1.

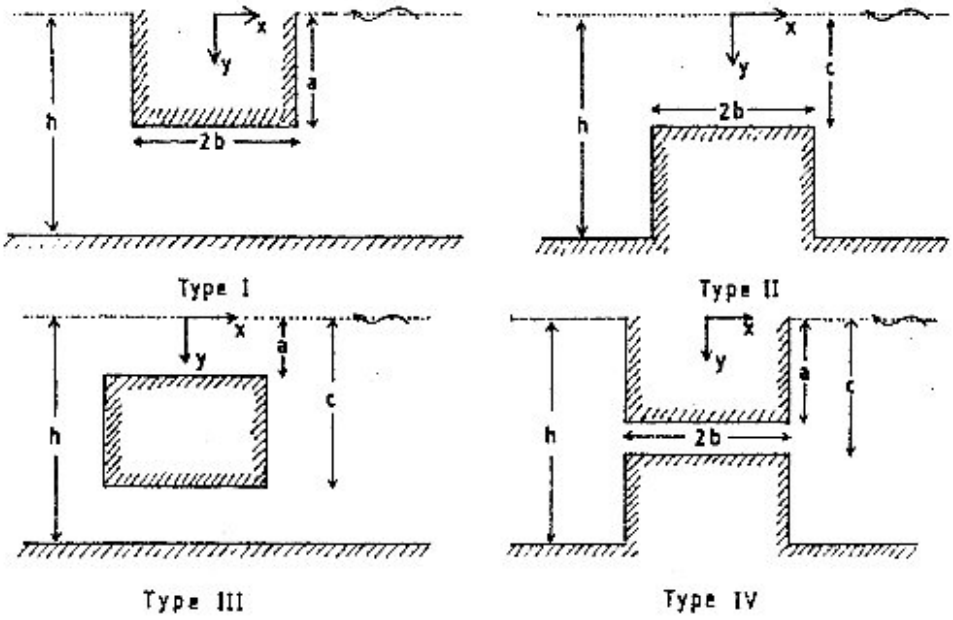

Figure 1. Definition sketch of the thick barriers.

Under the assumption of the linearised theory of water waves, a train of surface waves represented by the velocity potential $\mathrm{Re}\{\phi^{\mathrm{inc}}(x, y)\, \mathrm{e}^{-i\sigma t}\}$ is normally incident on a thick barrier of a particular configuration from a large distance on its right, $\phi^{\mathrm{inc}}(x, y)$ being given by

$$\phi^{\mathrm{inc}}(x, y) = \frac{2\cosh k_0(h - y)\, \mathrm{e}^{-ik_0(x-b)}}{\cosh k_0 h}, \tag{2.1}$$

where k_0 is the unique real positive root of the transcendental equation

$$k \tanh kh = K \tag{2.2}$$

with $K = \sigma^2/g$, σ being the circular frequency of the incoming wave train, g being the acceleration due to gravity. Let the resulting motion in the fluid be described by the velocity potential $\mathrm{Re}\{\phi(x, y)\, \mathrm{e}^{-i\sigma t}\}$, then $\phi(x, y)$ satisfies

$$\nabla^2\phi = 0 \quad \text{in the fluid region,} \tag{2.3}$$

$$K\phi + \phi_y = 0 \quad \text{on } y = 0, \begin{cases} |x| > b & \text{for type I, IV barrier,} \\ |x| < \infty & \text{for type II, III barrier,} \end{cases} \tag{2.4}$$

$$\phi_x = 0 \quad \text{on } x = \pm b, \qquad y \in L_j \quad \text{for type } j \text{ barrier } (j = 1, 2, 3, 4), \tag{2.5}$$

$$r^{1/3}\nabla\phi \quad \text{is bounded as } r \to 0, \tag{2.6}$$

where r is the distance from a submerged edge of the thick barrier,

$$\phi_y = 0 \quad \text{on } y = l_j, \qquad |x| < b \quad \text{for type } j \text{ barrier } (j = 1, 2, 3, 4), \tag{2.7}$$

$$\phi_y = 0 \text{ on } y = h, \begin{cases} |x| < \infty & \text{for type I, III barrier,} \\ |x| > b & \text{for type II, IV barrier} \end{cases} \tag{2.8}$$

and finally,

$$\phi(x, y) \sim \begin{cases} \phi^{\text{inc}}(x, y) + R\phi^{\text{inc}}(-x, y) & \text{as } x \to \infty, \\ T\phi^{\text{inc}}(x, y) & \text{as } x \to -\infty, \end{cases} \tag{2.9}$$

where R and T are the reflection and transmission coefficients (complex) and are to be determined for each barrier configuration. In Equation (2.7), $l_1 = a$; $l_2 = c$; $l_3 = a, c$ and $l_4 = a, c$ corresponding to type I, II, III and IV barrier configurations depicted in Figure 1.

3. The method of solution

Due to geometrical symmetry of the thick barrier about $x = 0$, it is convenient to split $\phi(x, y)$ into a symmetric and antisymmetric parts $\phi^s(x, y)$ and $\phi^a(x, y)$, respectively, so that

$$\phi(x, y) = \phi^s(x, y) + \phi^a(x, y), \tag{3.1}$$

where

$$\phi^s(-x, y) = \phi^s(x, y), \qquad \phi^a(-x, y) = -\phi^a(x, y). \tag{3.2}$$

Thus, we may restrict our analysis to the region $x \geqslant 0$ only. Now $\phi^{s,a}(x, y)$ satisfy Equations (2.3) to (2.8) together with

$$\phi^s_x(0, y) = 0, \qquad \phi^a(0, y) = 0, \quad 0 < y < h. \tag{3.3}$$

Let the behaviour of $\phi^{s,a}(x, y)$ for large x be represented by

$$\phi^{s,a}(x, y) \sim \frac{\cosh k_0(h - y)}{\cosh k_0 h} \left\{ e^{-ik_0(x-b)} + R^{s,a}\, e^{ik_0(x-b)} \right\} \quad \text{as } x \to \infty \tag{3.4}$$

where R^s and R^a are unknown constants. By using Equations (2.9) we find that, these constants are related to R and T by the equations

$$R, T = \tfrac{1}{2}(R^s \pm R^a)\, e^{-2ik_0 b}. \tag{3.5}$$

Now the eigenfunction expressions of $\phi^{s,a}(x, y)$ satisfying Equations (2.3) to (2.5), (2.7), (2.8), (3.3) and (2.4) (for $(x > b)$) in the different regions for each barrier configuration are given below.

Region I ($x > b,\ 0 < y < h$):

$$\phi^{s,a}(x,y) = \frac{\cosh k_0(h-y)}{\cosh k_0 h}\left\{e^{-ik_0(x-b)} + R^{s,a}\,e^{ik_0(x-b)}\right\} + \sum_{n=1}^{\infty} A_n^{s,a}\cos k_n(h-y)\,e^{-k_n(x-b)}, \tag{3.6}$$

where k_n ($n = 1, 2, \ldots$) are the real positive roots of the equation

$$k\tan kh + K = 0. \tag{3.7}$$

Region II ($0 < x < b,\ y \in \overline{L} \equiv \overline{L}_j = (0,h) - L_j,\ j = 1,2,3,4$):

For $y \in \overline{L}_1 = (a,h)$, $\phi^s(x,y)$ and $\phi^a(x,y)$ are given by

$$\begin{pmatrix}\phi^s(x,y)\\ \phi^a(x,y)\end{pmatrix} = \begin{pmatrix}0\\ B_0^a x\end{pmatrix} + \sum_{n=1}^{\infty}\begin{pmatrix}B_n^s\cosh\frac{n\pi x}{h-a}\\ B_n^a\sinh\frac{n\pi x}{h-a}\end{pmatrix}\cos\frac{n\pi(y-a)}{h-a}. \tag{3.8}$$

A nonzero constant term in the expansion of $\phi^s(x,y)$ is omitted here as its presence does not affect the calculation of the reflection coefficient by the present method. This is explained in detail in Appendix IV. However, there is no reason to believe that this constant is zero in general. If its value is required (for example, to determine the vertical force on a barrier) then it may be calculated by the method given in Appendix IV.

For $y \in \overline{L}_2 = (0,c)$, $\phi^s(x,y)$ and $\phi^a(x,y)$ are given by

$$\begin{pmatrix}\phi^s(x,y)\\ \phi^a(x,y)\end{pmatrix} = \begin{pmatrix}C_0^s\cos\alpha_0 x\\ C_0^a\sin\alpha_0 x\end{pmatrix}\frac{\cos\alpha_0(c-y)}{\cosh\alpha_0 c} + \sum_{n=1}^{\infty}\begin{pmatrix}C_n^s\cosh\alpha_n x\\ C_n^a\sinh\alpha_n x\end{pmatrix}\cos\alpha_n(c-y), \tag{3.9}$$

where $\pm\alpha_0,\ \pm i\alpha_n$ ($n = 1, 2, \ldots$) are the roots of the equation

$$\alpha\tanh\alpha c = K. \tag{3.10}$$

For $y \in \overline{L}_3 = (0,a) + (c,h)$, $\phi^{s,a}(x,y)$ will have two types of expansions depending on whether $0 < y < a$ or $c < y < h$. For $0 < y < a$, the expansions of $\phi^{s,a}(x,y)$ are similar to (3.9) with $C_n^{s,a}$ replaced by $D_n^{s,a}$, α_n replaced by β_n ($n = 0, 1, 2, \ldots$) and c replaced by a, where $\pm\beta_0,\ \pm i\beta_n$ ($n = 1, 2, \ldots$) are the roots of the equation

$$\beta\tanh\beta a = K. \tag{3.11}$$

For $c < y < h$, the expansions of $\phi^{s,a}(x,y)$ are similar to (3.8) with B_n^s replaced by E_n^s ($n = 1, 2, \ldots$), B_n^a replaced by E_n^a ($n = 0, 1, 2, \ldots$) and a replaced by c.

For $y \in \overline{L}_4 = (a,c)$, the expansions of $\phi^{s,a}(x,y)$ are the same as given by Equation (3.8) with B_n^s replaced by H_n^s ($n = 1, 2, \ldots$), B_n^a replaced H_n^a ($n = 0, 1, 2, \ldots$) and h replaced by c.

Let us now define

$$\phi_x^{s,a}(b+0,\, y) = f^{s,a}(y), \quad 0 < y < h. \tag{3.12}$$

Then

$$f^{s,a}(y) = 0 \quad \text{for } y \in L \equiv L_j, \tag{3.13}$$

and

$$\phi_x^{s,a}(b-0,\, y) = f^{s,a}(y) \quad \text{for } y \in \overline{L} \equiv (0,h) - L. \tag{3.14}$$

Also, due to the edge condition described by (2.6), we must have the requirement that

$$f^{s,a}(y) = 0(|y-l|^{-1/3}) \quad \text{as } y \to l \tag{3.15}$$

where $l \equiv l_j$ for barrier of type j ($j = 1, 2, 3, 4$).

Use of the expansion (3.6) for $\phi^{s,a}(x, y)$ in Equation (3.12) followed by Havelock's [19] inversion formula, produces, after noting the condition (3.13),

$$1 - R^{s,a} = \frac{4i\cosh k_0 h}{\delta_0} \int_{\overline{L}} f^{s,a}(y) \cosh k_0(h-y)\, \mathrm{d}y \tag{3.16}$$

with

$$\delta_0 = 2k_0 h + \sinh 2k_0 h, \qquad A_n^{s,a} = -\frac{4}{\delta_n} \int_{\overline{L}} f^{s,a}(y) \cos k_n(h-y)\, \mathrm{d}y$$

with

$$\delta_n = 2k_n h + \sin 2k_n h \quad (n = 1, 2, \ldots). \tag{3.17}$$

Substituting the expansions (3.8) for $\phi^{s,a}(x, y)$ in Equation (3.14) and using Fourier cosine inversion, we find that $f^s(y)$ for type I barrier satisfies the condition

$$\int_a^h f^s(y)\, \mathrm{d}y = 0, \tag{3.18}$$

and the constants B_0^a, $B_n^{s,a}$ ($n = 1, 2, \ldots$) are obtained as

$$B_0^a = \frac{1}{h-a} \int_a^h f^a(y)\, \mathrm{d}y, \tag{3.19}$$

$$B_n^{s,a} = \frac{2}{n\pi} \left(\frac{1}{\sinh \frac{n\pi b}{h-a}}, \frac{1}{\cosh \frac{n\pi b}{h-a}} \right) \int_a^h f^{s,a}(y) \cos \frac{n\pi(y-a)}{h-a}\, \mathrm{d}y. \tag{3.20}$$

The constants $C_n^{s,a}$ ($n = 0, 1, 2, \ldots$) appearing in Equations (3.9) are related to $f^{s,a}(y)$ for type II barrier by the following expressions obtained by using Havelock's inversion formula in Equation (3.14) for $0 < y < c$:

$$C_0^{s,a} = \frac{4\cosh \alpha_0 c}{\gamma_0} \left(-\frac{1}{\sin \alpha_0 b}, \frac{1}{\cos \alpha_0 b} \right) \int_0^c f^{s,a}(y) \cosh \alpha_0(c-y)\, \mathrm{d}y \tag{3.21}$$

with

$$\gamma_0 = 2\alpha_0 c + \sinh 2\alpha_0 c,$$

$$C_n^{s,a} = \frac{4}{\gamma_n}\left(\frac{1}{\sinh\alpha_n b}, \frac{1}{\cosh\alpha_n b}\right)\int_0^c f^{s,a}(y)\cos\alpha_n(c-y)\,\mathrm{d}y$$

with

$$\gamma_n = 2\alpha_n c + \sin 2\alpha_n c \quad (n = 1, 2, \ldots) \tag{3.22}$$

For type III barrier, we derive expressions for $D_n^{s,a}$ from $C_n^{s,a}$ by replacing α_n by β_n and γ_n by ϵ_n $(n = 0, 1, 2, \ldots)$

$$\epsilon_0 = 2\beta_0 a + \sinh 2\beta_0 a, \qquad \epsilon_n = 2\beta_n a + \sinh 2\beta_n a \quad (n = 1, 2, \ldots) \tag{3.23}$$

and E_n^s is derived from B_n^s $(n = 1, 2, \ldots)$; we derive E_n^a from B_n^a $(n = 0, 1, 2, \ldots)$ by replacing a by c and in this case $f^s(y)$ $(c < y < h)$ must satisfy

$$\int_c^h f^s(y)\,\mathrm{d}y = 0. \tag{3.24}$$

For type IV barrier, H_n^s is derived from B_n^s $(n = 1, 2, \ldots)$ and we derive H_n^a from B_n^a $(n = 0, 1, 2, \ldots)$ by replacing h by c and in this case $f^s(y)$ $(a < y < c)$ must satisfy

$$\int_a^c f^s(y)\,\mathrm{d}y = 0. \tag{3.25}$$

It may be noted that the condition (3.18) or (3.24) or (3.25) for $f^s(y)$ corresponding to type I or type III or type IV barrier, may be regarded as the compatibility condition for the existence of solution in the region $|x| < b$, $y \in \overline{L}_1$ or (c, h) or $\overline{L}_4$. This condition plays an important role in the choice of the basis functions for $f^s(y)$ $(y \in \overline{L}_1$ or (c, h) or $\overline{L}_4)$ (see Appendix II).

Now matching of $\phi^{s,a}(x, y)$ across the line $x = b$ through the right corner points of the gap, or gaps, gives rise to the relations

$$\phi^{s,a}(b + 0, y) = \phi^{s,a}(b - 0, y), \quad y \in \overline{L}, \tag{3.26}$$

which ultimately produce the integral equations

$$\int_{\overline{L}} F^{s,a}(u)\mathcal{M}^{s,a}(y, u)\,\mathrm{d}u = \frac{\cosh k_0(h - y)}{\cosh k_0 h}, \quad y \in \overline{L}, \tag{3.27}$$

where

$$F^{s,a}(y) = \frac{4\cosh^2 k_0 h}{\delta_0(1 + R^{s,a})}\, f^{s,a}(y), \quad y \in \overline{L}, \tag{3.28}$$

and $\mathcal{M}^{s,a}(y, u)$ $(y, u \in \overline{L})$ are real and symmetric in y and u, and their expressions for $\overline{L} = \overline{L}_j$ $(j = 1, 2, 3, 4)$ are given in Appendix I.

If we now define the constants $C^{s,a}$ by

$$C^{s,a} = -i\frac{1 - R^{s,a}}{1 + R^{s,a}}, \tag{3.29}$$

then, by using the relations (3.16) and (3.28), we find that

$$\int_{\overline{L}} F^{s,a}(y)\frac{\cosh k_0(h - y)}{\cosh k_0 h}\,\mathrm{d}y = C^{s,a}. \tag{3.30}$$

It is important to note that $F^{s,a}(y)$ and $C^{s,a}$ are all real quantities. Thus, if the integral Equations (3.27) are solved, then these solutions can be utilized to obtain $C^{s,a}$ from the relation (3.30), and these in turn produce the actual reflection and transmission coefficients $|R|$ and $|T|$, respectively, from the relations

$$|R| = \frac{|1 + C^s C^a|}{\Delta}, \qquad |T| = \frac{|C^s - C^a|}{\Delta}$$

with

$$\Delta = \{1 + (C^s)^2 + (C^a)^2 + (C^s C^a)^2\}^{1/2}, \tag{3.31}$$

which are obtained from Equations (3.29) and (3.5).

To solve the integral Equations (3.27), we adopt a Galerkin approach. The functions $F^{s,a}(y)$ are approximated as

$$F^{s,a}(y) \approx \mathcal{F}^{s,a}(y), \quad y \in \overline{L}, \tag{3.32}$$

where $\mathcal{F}^{s,a}(y)$ have multi-term Galerkin expansions in terms of suitable basis functions. We note that $\overline{L}_1, \overline{L}_2, \overline{L}_4$ are single intervals while $\overline{L}_3$ consists of two disjoint intervals. For the single interval $\overline{L}_j$ $(j = 1, 2, 4)$, $\mathcal{F}^{s,a}(y)$ are expressed as

$$\mathcal{F}^{s,a}(y) = \sum_{n=0}^{N} a_n^{s,a} f_n^{s,a}(y), \quad y \in \overline{L}_j \ (j = 1, 2, 4), \tag{3.33}$$

and, for the double interval $\overline{L}_3 = (0, a) + (c, h)$, $\mathcal{F}^{s,a}(y)$ are expressed as

$$\mathcal{F}^{s,a}(y) = \begin{cases} \displaystyle\sum_{n=0}^{N} a_n^{s,a} p_n^{s,a}(y), & 0 < y < a, \\ \displaystyle\sum_{n=0}^{N} b_n^{s,a} q_n^{s,a}(y), & c < y < h, \end{cases} \tag{3.34}$$

where the basis functions $f_n^{s,a}(y)$ for $y \in \overline{L}_j$ $(j = 1, 2, 4)$ and $p_n^{s,a}(y)$ for $0 < y < a$, $q_n^{s,a}(y)$ for $c < y < h$ are given in Appendix II, and $a_n^{s,a}$, $b_n^{s,a}$ are unknown constants to be found separately for each type of barrier as described below.

When $\overline{L} = \overline{L}_j\,(j = 1, 2, 4)$, we substitute the expansion (3.33) in Equations (3.27), multiply by appropriate $f_m^{s,a}(y)$ and integrate over $\overline{L}$ to obtain the linear systems

$$\sum_{n=0}^{N} a_n^{s,a} K_{mn}^{s,a} = d_m^{s,a}, \quad m = 0, 1, 2, \ldots, N, \tag{3.35}$$

where

$$K_{mn}^{s,a} = \int_{\overline{L}} \int_{\overline{L}} \mathcal{M}^{s,a}(y, u) f_n^{s,a}(u) f_m^{s,a}(y)\, \mathrm{d}u\, \mathrm{d}y, \quad m, n = 0, 1, 2, \ldots, N, \tag{3.36}$$

$$d_m^{s,a} = \int_{\overline{L}} \frac{\cosh k_0(h - y)}{\cosh k_0 h} f_m^{s,a}(y)\, \mathrm{d}y, \quad m = 0, 1, 2, \ldots, N. \tag{3.37}$$

For each $\overline{L}_j\,(j = 1, 2, 4)$, the integrals in the relations (3.36) and (3.37) can be evaluated explicitly, and these are given in Appendix III. Thus the constants $a_n^{s,a}\,(n = 0, 1, \ldots N)$ are now obtained by solving the linear Equations (3.35) for each of type I, type II and type IV barrier. The relations (3.30) produce

$$C^{s,a} = \sum_{n=0}^{N} a_n^{s,a} d_n^{s,a}, \tag{3.38}$$

so that $C^{s,a}$ are now found for each of the type I, type II and type IV barrier.

When $L = \overline{L}_3 = (0, a) + (c, h)$, we substitute the expansions (3.34) in Equations (3.27) for $\overline{L} = \overline{L}_3$, multiply first by $p_m^{s,a}(y)\,(0 < y < a)$ and then by $q_m^{s,a}(y)\,(c < y < h)$ and integrate over $(0, a)$ and (c, h), respectively, to obtain the linear systems

$$\sum_{n=0}^{N} a_n^{s,a} \begin{pmatrix} G_{mn}^{s,a} \\ P_{mn}^{s,a} \end{pmatrix} + \sum_{n=0}^{N} b_n^{s,a} \begin{pmatrix} H_{mn}^{s,a} \\ Q_{mn}^{s,a} \end{pmatrix} = \begin{pmatrix} d_m^{(1)_{s,a}} \\ d_m^{(2)_{s,a}} \end{pmatrix}, \quad m = 0, 1, \ldots N, \tag{3.39}$$

where

$$\begin{aligned}
G_{mn}^{s,a} &= \int_0^a \left\{ \int_0^a \mathcal{M}^{s,a}(y, u) p_n^{s,a}(u)\, \mathrm{d}u \right\} p_m^{s,a}(y)\, \mathrm{d}y, \\
H_{mn}^{s,a} &= \int_0^a \left\{ \int_c^h \mathcal{M}^{s,a}(y, u) q_n^{s,a}(u)\, \mathrm{d}u \right\} p_m^{s,a}(y)\, \mathrm{d}y, \\
P_{mn}^{s,a} &= \int_c^h \left\{ \int_0^a \mathcal{M}^{s,a}(y, u) p_n^{s,a}(u)\, \mathrm{d}u \right\} q_m^{s,a}(y)\, \mathrm{d}y, \\
Q_{mn}^{s,a} &= \int_c^h \left\{ \int_c^h \mathcal{M}^{s,a}(y, u) q_n^{s,a}(u)\, \mathrm{d}u \right\} q_m^{s,a}(y)\, \mathrm{d}y,
\end{aligned} \tag{3.40}$$

so that

$$P_{nm}^{s,a} = H_{mn}^{s,a},$$

and

$$d_m^{(1)s,a} = \int_0^a \frac{\cosh k_0(h-y)}{\cosh k_0 h} p_m^{s,a}(y)\,\mathrm{d}y,$$

$$d_m^{(2)s,a} = \int_c^h \frac{\cosh k_0(h-y)}{\cosh k_0 h} q_m^{s,a}(y)\,\mathrm{d}y. \tag{3.41}$$

The integrals in the relations (3.40) and (3.41) can be evaluated explicitly and these are given in Appendix III. Thus for type III barrier, $a_n^{s,a}$ and $b_n^{s,a}$ $(n = 0, 1, \ldots N)$ in the relations (3.34) are obtained by solving the linear systems (3.39) and $C^{s,a}$ are approximated as

$$C^{s,a} = \sum_{n=0}^{N} \{a_n^{s,a} d_n^{(1)s,a} + b_n^{s,a} d_n^{(2)s,a}\}. \tag{3.42}$$

4. Numerical results

Since $|R|^2 + |T|^2 = 1$, we mostly confine our attention to the reflection coefficient $|R|$ only. Multi-term Galerkin approximations are used to obtain a numerical estimate for $|R|$. For each barrier configuration we have to compute infinite series of the form $K_{mn}^{s,a}$. These series are computed numerically by truncation. A six-figure accuracy is achieved by taking 200 terms in each series. However, the accuracy can be further increased by following a numerical procedure suggested by Porter and Evans [9] in the computation of series of this type. This is not pursued here.

We display a representative set of numerical estimates for $|R|$ for the four type of barriers in Table 1, taking $N = 0, 1, 2, 3, 4$ and 5 in the $(N + 1)$-term Galerkin approximations and some particular values of the different parameters and the wave number. It is observed from this table that the computed results for $|R|$ converge very rapidly with N, and for $N \geqslant 3$ an accuracy of almost six decimal places is achieved. It appears that the present numerical procedure for the numerical computation of $|R|$ is quite efficient.

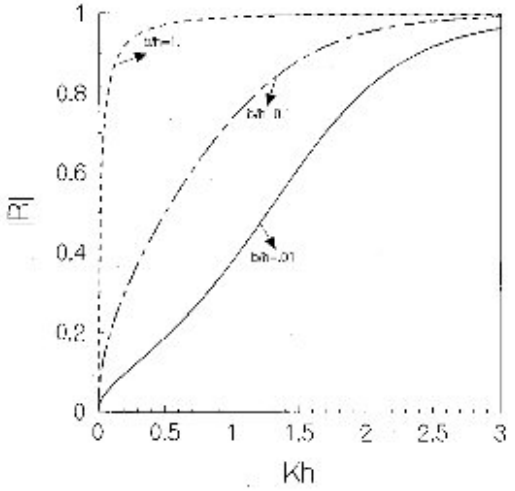

Figure 2a. Reflection coefficient for type I barrier, $a/h = 1{\cdot}2$.

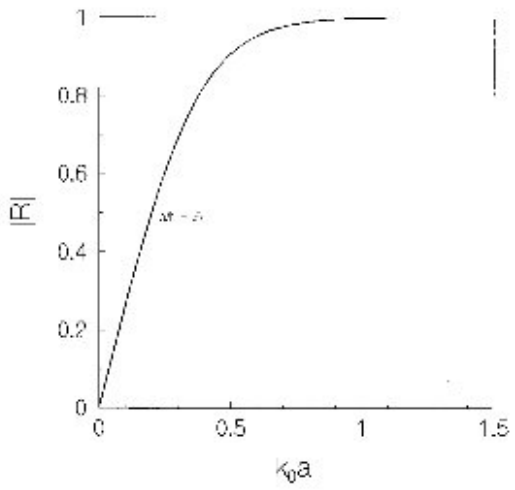

Figure 2b. Reflection coefficient vs $k_0 a$ for type I barrier, $a/h = 0{\cdot}5$.

Table 1. Reflection coefficient $|R|$.

Kh	$N=0$	$N=1$	$N=2$	$N=3$	$N=4$	$N=5$
Type I Barrier $a/h=0{\cdot}2,\ b/h=0{\cdot}5$						
0·2	0·783791	0·778117	0·778024	0·778019	0·778019	0·778019
1·0	0·968121	0·967934	0·967934	0·967934	0·967934	0·967934
1·8	0·993855	0·992526	0·992543	0·992543	0·992543	0·992543
Type II Barrier $c/h=0{\cdot}5,\ b/h=0{\cdot}5$						
0·2	0·446081	0·441869	0·441811	0·441808	0·441808	0·441808
1·0	0·007353	0·006603	0·006675	0·006679	0·006679	0·006679
1·8	0·364916	0·361848	0·361618	0·361602	0·361602	0·361602
Type III Barrier $a/h=0{\cdot}2,\ c/h=0{\cdot}4,\ b/h=0{\cdot}5$						
0·2	0·648346	0·638165	0·637977	0·637966	0·637965	0·637965
1·0	0·924199	0·925042	0·925058	0·925058	0·925058	0·925058
1·8	0·865962	0·866637	0·866616	0·866616	0·866616	0·866616
Type IV Barrier $a/h=0{\cdot}2,\ c/h=0{\cdot}4,\ b/h=0{\cdot}5$						
0·2	0·981698	0·981676	0·981676	0·981676	0·981676	0·981676
1·0	0·996937	0·996358	0·996358	0·996358	0·996358	0·996358
1·8	0·998484	0·998319	0·998319	0·998319	0·998319	0·998319

For a *surface-piercing thick barrier* (type I barrier), the computed results for $|R|$ are plotted in Figure 2(a) against the wave number Kh for $a/h = 0{\cdot}2$ and $b/h = 0{\cdot}01, 0{\cdot}1, 1{\cdot}0$. It is observed from this figure that, for a fixed value of the wave number Kh, $|R|$ increases with the thickness of the barrier. Also, $|R|$ increases asymptotically to unity as the wave number becomes large, which is plausible, since, for large wave number, the incident wave train is confined within a thin layer below the free surface and as such most of the incident wave energy is reflected back by the surface-piercing barrier. Also, when the thickness is equal to water depth, $|R|$ becomes near unity for moderately large values of the wave number. In order to compare our results with those of Mei and Black [28], in Figure 2(b) we have drawn $|R|$ against k_0a for $b/h = 0{\cdot}5$, $a/h = 0{\cdot}5$. This curve almost coincides with the corresponding curve given in Figure 6 of Mei and Black [28].

For a *bottom-standing thick barrier* (type II barrier), $|R|$ is depicted in Figure 3 against Kh for $c/h = 0{\cdot}5$ and $b/h = 0{\cdot}01, 1{\cdot}0, 2{\cdot}0$ and $5{\cdot}0$. It is observed that, when the barrier is comparatively thin ($b/h = 0{\cdot}01$), $|R|$ first increases and then decreases asymptotically to zero with the increase of the wave number. This is the usual behaviour of the reflection coefficient for an infinitely thin barrier. However, as the thickness increases, $|R|$ starts fluctuating and the fluctuations become rapid as the thickness of the barrier further increases. For very large wave number $|R|$ becomes zero asymptotically, which is obvious, since the incident wave train then does not penetrate enough below the free surface to feel the presence of the submerged barrier. The oscillatory behaviour of $|R|$ is due to interaction between the two ends of the thick barrier. Also, $|R|$ assumes zero values for a number of frequencies of the incident wave train. This type of behaviour of $|R|$ is consistent with the study of Mei and Black [28] for bottom-standing barriers. The curve of $|R|$ for $b/h = 5{\cdot}0$ (large horizontal breadth) may be identified with the curve given by Newman [30] for a long rectangular obstacle in which case the depth

is infinite, except at the obstacle. Except for the low-frequency region, the qualitative nature of the curves is similar. As the frequency parameter tends to zero, $|R|$ tends to unity for deep water (Newman's figure), while in the case of water of finite depth, $|R|$ tends to zero (Figure 3 here). This is the so-called low-frequency paradox mentioned by Tuck [20].

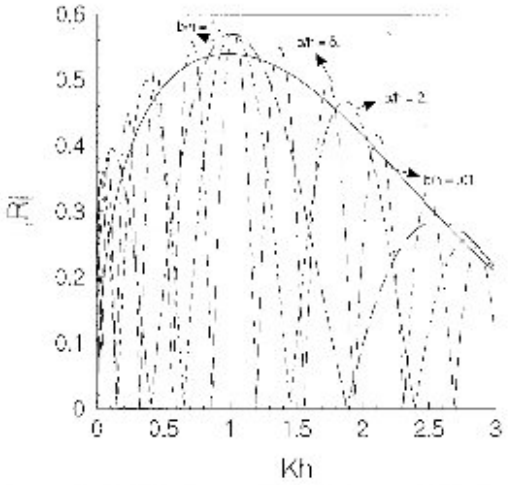

Figure 3. Reflection coefficient for type II barrier, $c/h = 0{\cdot}5$.

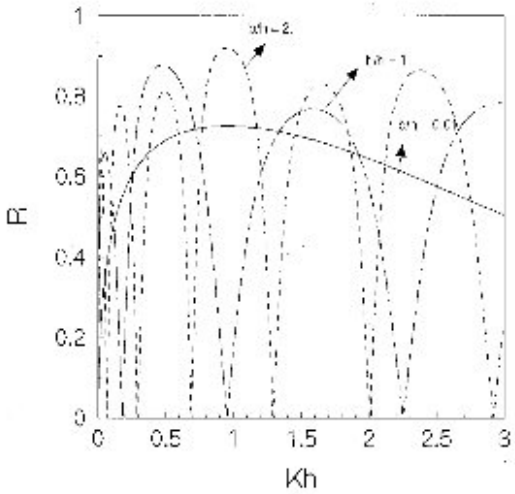

Figure 4. Reflection coefficient for type III barrier, $a/h = 0{\cdot}2, c/h = 0{\cdot}4$.

For a *submerged thick rectangular block* (type III barrier), $|R|$ is plotted against Kh in Figure 4 for $a/h = 0{\cdot}2$, $c/h = 0{\cdot}4$ and $b/h = 0{\cdot}01$, $1{\cdot}0$ and $2{\cdot}0$. Here also the thickness of the barrier affects $|R|$ significantly. For small thickness ($b/h = 0{\cdot}01$), as in the case of a type II barrier, $|R|$ first increases and then decreases to zero asymptotically as the wave number increases. As the thickness increases, $|R|$ starts oscillating and the occurrence of a number of zeros of $|R|$ is observed. The number of oscillations increases with the increase of thickness as in the case of type II barrier. By looking at Figures 3 and 4, we also observe that there is some similarity in the qualitative behaviour of $|R|$ against the wave number for barriers of type II and type III. In fact, if the gap between the lower end of a type III barrier and the bottom is made very small, then this would behave almost like a bottom-standing barrier (type II) although there will still be some transmission through the very small gap. In Figure 5 for a type III barrier, we depicte $|R|$, against Kh taking $b/h = 0{\cdot}01$, $1{\cdot}0$, $a/h = 0{\cdot}5$, $c/h = 0{\cdot}999$, so that the gap between the barrier and the bottom becomes very small. Also for a type II barrier, we depicte $|R|$, in the same figure taking $b/h = 0{\cdot}01$, $1{\cdot}0$, $c/h = 0{\cdot}5$. It is observed that the curve of $|R|$ for type III barrier with $b/h = 0{\cdot}01$ lies slightly below the curve of $|R|$ for type II barrier with $b/h = 0{\cdot}01$. The small difference in the two curves is due to some small transmission of the incident wave energy below the type III barrier as there is still some gap, although very narrow, between its lower end and the bottom. However for $b/h = 1{\cdot}0$, the two curves practically coincide. This is due to considerable increase in the thickness of the barriers.

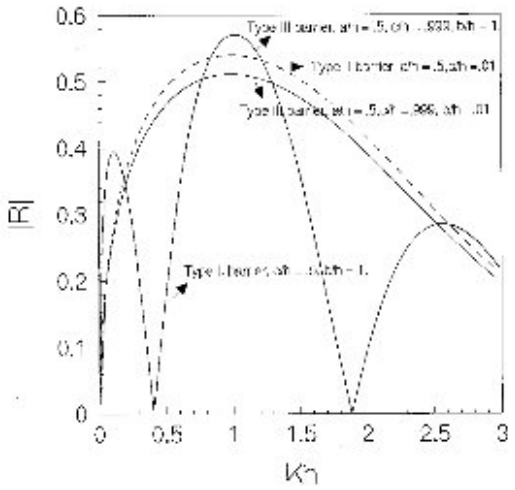

Figure 5. Reflection coefficient vs wave number.

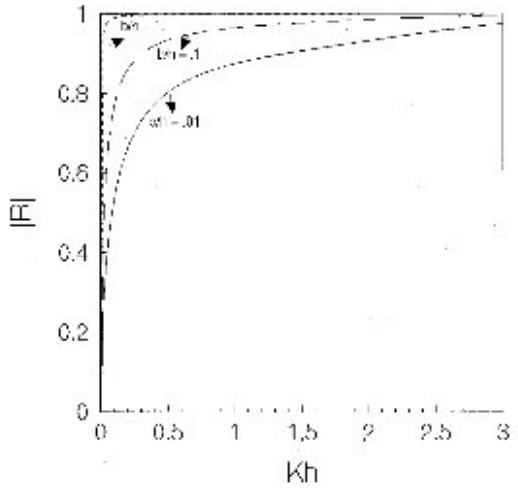

Figure 6. Reflection coefficient for type IV barrier, $a/h = 0{\cdot}2, c/h = 0{\cdot}4$.

Finally, for a *thick vertical wall with a submerged gap* (type IV barrier), $|R|$ is depicted graphically against Kh in Figure 6 for $a/h = 0{\cdot}2$, $c/h = 0{\cdot}4$ and $b/h = 0{\cdot}01, 0{\cdot}1, 1{\cdot}0$. It is observed from this figure that $|R|$ steadily increases as the wave number Kh increases and asymptotically becomes unity for large Kh. Also, for a fixed wave number, $|R|$ increases as the thickness increases. It is interesting to observe that, when thickness is equal to the water depth ($b/h = 1{\cdot}0$), $|R|$ very quickly becomes near unity for even moderate values of the wave number. A similar behaviour of $|R|$ is also observed for type I barrier, although in that case the wave number is moderately large. Again, from the Figures 2(a) and 6 it is observed that there is some similarity in the qualitative behaviour of $|R|$ for the type I and type IV barriers. In both cases $|R|$ increases asymptotically to unity and there is no oscillation in $|R|$. This is due to the fact that both barriers are surface piercing. In fact, if we confine the lower part of the type IV barrier near the bottom by making c/h nearly unity, then it assumes the form of a type I barrier and thus we expect that the curves of $|R|$ for the two types of barrier in that case should be very near to each other. In Figure 7, for a type IV barrier, $|R|$ is plotted against Kh for $a/h = 0{\cdot}2, b/h = 0{\cdot}1, c/h = 0{\cdot}999$ and $|R|$ for a type I barrier is plotted for the same values of a/h and b/h. The two curves almost coincide. Finally, to compare our results for a type IV barrier with the results of Packham and Williams [21] for a submerged *narrow* gap in an infinitely thin wall, for a type IV barrier, we plot $|T|^2 \equiv 1 - |R|^2$ in Figure 8 against $KH (H = (a + c)/2)$, taking $c/h = 0{\cdot}86, a/h = 0{\cdot}74$ and $b/h = 0{\cdot}01, 0{\cdot}001$, so that the thickness of the barrier is small and the gap is narrow. The qualitative behaviour of the two curves depicting $|T|^2$ against KH is observed to be very similar to the curve for $|T|^2$ (the upper most curve in Figure 1 of [21]) given by Packham and Williams [21] for an infinitely thin barrier. It may be noted that for deep water $|T|^2 \to 0$ as $KH \to 0$, while for water of finite depth $|T|^2 \to 1$ as $KH \to 0$ and the latter is observed in Figure 8. This is the so called low-frequency paradox mentioned earlier.

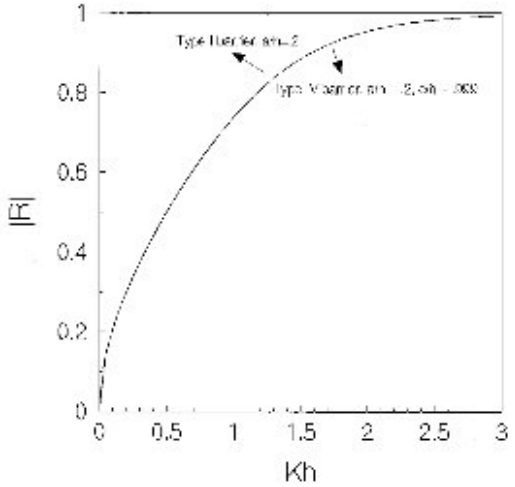

Figure 7. Reflection coefficient vs wave number, $b/h = 0{\cdot}1$.

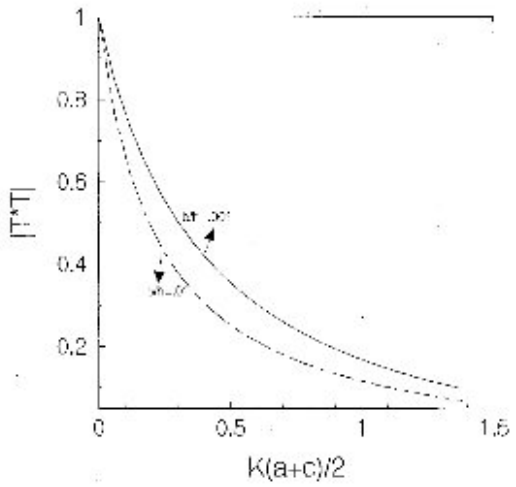

Figure 8. Type IV barrier, transmission coefficient vs $K(a+c)/2$.

For all the four types of thick rectangular vertical barriers it is observed that the long-wave limit of the reflection coefficient $|R|$ is zero as is evident from the Figures 2–7. Martin and Dalrymple [31] and McIver [32] confirmed, by using the method of matched asymptotic expansions, that the long-wave limit of $|R|$ for any obstacle is zero. This provides a partial check on the correctness of the numerical method utilized here.

5. Conclusion

The method of multi-term Galerkin approximations in terms of ultraspherical Gegenbauer polynomials has been utilized here to obtain very accurate numerical estimates for the reflection coefficient in the water wave scattering problems involving thick rectangular barriers of four different geometrical configurations in water of uniform finite depth. By choosing only four terms in the Galerkin approximations, we achieve almost six-figure accuracy in the numerical estimate for the reflection coefficient. The numerical results are illustrated graphically, and some results are compared with known results available in the literature, for which good agreement is achieved. The thickness of a barrier affects the reflection coefficient considerably and thus the thickness plays a significant role in the modelling of breakwaters.

Acknowledgement

The authors thank the referees and Professor H. K. Kuiken, Editor-in-Chief, for their constructive suggestions and comments to improve two earlier versions of the paper in the present form. A comment from one of the referees has led to the introduction of the Appendix IV and the inclusion of reference [33]. This work is supported by the National Board for Higher Mathematics, Bombay and CSIR New Delhi.

Appendix I. Expressions for $\mathcal{M}^{s,a}(y,u)$

(i) *For* $y, u \in \overline{L}_1 = (a, h)$, we find that $\mathcal{M}^s(y, u)$ is given by

$$\mathcal{M}^s(y,u) = \frac{\delta_0}{\cosh^2 k_0 h}\left[\sum_{n=1}^{\infty}\left\{\frac{\cos k_n(h-y)\cos k_n(h-u)}{\delta_n} + \frac{1}{2n\pi}\coth\frac{n\pi b}{h-a}\cos\frac{n\pi(y-a)}{h-a}\cos\frac{n\pi(u-a)}{h-a}\right\}\right]. \tag{A1.1}$$

The expression for $\mathcal{M}^a(y, u)$ is obtained by replacing 'coth' by 'tanh'in the relation (A1.1) and inserting an extra term $b/4(h-a)$ inside the square bracket.

(ii) *For* $y, u \in \overline{L}_2 = (0, c)$, we find that $\mathcal{M}^s(y, u)$ is given by

$$\mathcal{M}^s(y,u) = \frac{\delta_0}{\cosh^2 k_0 h}\left[\sum_{n=1}^{\infty}\left\{\frac{\cos k_n(h-y)\cos k_n(h-u)}{\delta_n} + \frac{\coth\alpha_n b\cos\alpha_n(c-y)\cos\alpha_n(c-u)}{\gamma_n} - \cot\alpha_0 b\frac{\cos\alpha_0(c-y)\cos\alpha_0(c-u)}{\gamma_0}\right\}\right]. \tag{A1.2}$$

The expression for $\mathcal{M}^a(y, u)$ is obtained by replacing 'coth' by 'tanh' and '$-\cot$' by 'tan' in the relation (A1.2).

(iii) *For* $y, u \in \overline{L}_3 = (0, a) + (c, h)$.

For $y, u \in (0, a)$, $\mathcal{M}^s(y, u)$ is obtained from the relation (A1.2) by replacing c by a and similarly for $\mathcal{M}^a(y, u)$. For $y, u \in (c, h)$, $\mathcal{M}^s(y, u)$ is obtained from the relation (A1.1) by replacing a by c and similarly for $\mathcal{M}^a(y, u)$. For $y \in (0, a), u \in (c, h)$ and $y \in (c, h)$, $u \in (0, a)$,

$$\mathcal{M}^s(y,u) = \mathcal{M}^a(y,u) = \frac{\delta_0}{\cosh^2 k_0 h}\sum_{n=1}^{\infty}\frac{\cos k_n(h-y)\cos k_n(h-u)}{\delta_n}. \tag{A1.3}$$

(iv) *For* $y, u \in \overline{L}_4 = (a, c)$, $\mathcal{M}^s(y, u)$ is obtained from the relation (A1.1) by replacing h by c, and similarly for $\mathcal{M}^a(y, u)$.

Appendix II. The basis functions

The basis functions are to be chosen such that they satisfy the appropriate physical requirements and the final forms of various expressions occurring in the analysis become as simple as possible [29]. Since the horizontal velocity of the fluid near the corner point (b, l) of a thick barrier has a cubic-root singularity, derived by a simple conformal mapping argument for the flow of an ideal fluid around a corner, we expect that a basis function $f_n^{s,a}(y)$ must satisfy

$$f_n^{s,a}(y) \sim O(|y-l|)^{-1/3} \quad \text{as } y \to l. \tag{A2.1}$$

Porter (*cf.* Evans and Fernyhough [29]) suggested that a basis function which satisfies the requirement (A2.1), can be chosen in terms of ultraspherical Gegenbauer polynomials of order 1/6 with suitable weights. We give below the forms of the basis functions in various intervals along with the reasons for choosing such forms.

(i) $y \in \overline{L}_1 = (a, h)$.

In this case, the velocities $F^{s,a}(y)$ satisfy

$$F^{s,a}(y) \sim (y-a)^{-1/3} \quad \text{as } y \to a+0. \tag{A2.2}$$

Since $\phi_y^{s,a} = 0$ on $y = h$, $\phi^{s,a}$ and hence $F^{s,a}(y) \propto \phi_x^{s,a}(b, y)$ can be continued as an even function of y across $y = h$ *i.e.* it is an even function of $h - y$. Thus, the even continuous function $\{(h-a)^2 - (h-y)^2\}^{-1/3} F^{s,a}(y)$ can be expanded in (a, h) in terms of even ultraspherical Gegenbauer polynomials $C_{2m}^{1/6}(h - y/h - a)$. However, $F^s(y)$ has to satisfy the additional requirement that (see Equation (3.18))

$$\int_a^h F^s(y)\,\mathrm{d}y = 0. \tag{A2.3}$$

Noting the results

$$\int_a^h \frac{1}{\{(h-a)^2 - (h-y)^2\}^{1/3}(h-a)^{1/3}} C_{2m}^{1/6}\left(\frac{h-y}{h-a}\right)\mathrm{d}y$$

$$= \frac{1}{2}\int_{-1}^{1} (1-t^2)^{-1/3} C_{2m}^{1/6}(t)\,\mathrm{d}t = \begin{cases} 0 & \text{for } m > 0 \\ \frac{3\sqrt{\pi}\,\Gamma(\frac{2}{3})}{\Gamma(\frac{1}{6})} & \text{for } m = 0, \end{cases} \tag{A2.4}$$

we observe that the basis functions for $F^s(y)$ are to be chosen starting from a function which involves $C_2^{1/6}$. However, for $F^a(y)$ the basis functions start from $C_0^{1/6}$. Thus we choose the basis functions for $F^s(y)$ and $F^a(y)$ in the present case as

$$\begin{aligned} f_m^s(y) &= g_{m+1}^{(1)}(y) \quad m = 0, 1, 2, \ldots, \\ f_m^a(y) &= g_m^{(1)}(y) \quad m = 0, 1, 2, \ldots, \end{aligned} \tag{A2.5}$$

where

$$g_m^{(1)}(y) = \frac{2^{7/6}\Gamma(1/6)(2m)!}{\pi\Gamma(2m+\frac{1}{3})(h-a)^{1/3}\{(h-a)^2 - (h-y)^2\}^{1/3}} C_{2m}^{1/6}\left(\frac{h-y}{h-a}\right). \tag{A2.6}$$

(ii) $y \in \overline{L}_2 = (0, c)$.

In this case we have to consider the free-surface condition and the behaviour $F^{s,a}(y) \sim (c-y)^{-1/3}$ as $y \to c-0$ derived by considering the flow field near the corner point (b, c). Thus $F^{s,a}(y) \equiv F(y)$ in this case satisfies

$$KF(y) + F'(y) = 0, \quad y = 0, \tag{A2.7}$$

$$F(y) \sim (c-y)^{-1/3} \quad \text{as } y \to c-0. \tag{A2.8}$$

If we introduce $\widehat{F}(y)$ defined by

$$\widehat{F}(y) = F(y) - K\int_y^c F(u)\,\mathrm{d}u, \quad 0 < y < c \tag{A2.9}$$

then,

$$\widehat{F}'(y) = 0, \quad y = 0, \tag{A2.10}$$

$$\widehat{F}(y) \sim (c-y)^{-1/3} \quad \text{as } y \to c-0. \tag{A2.11}$$

The condition (A2.10) shows that $\widehat{F}(y)$ can be continued as an even function of y into $(-c, 0)$. Thus, because of the condition (A2.11), $(c^2-y^2)^{1/3}\widehat{F}(y)$ can be expanded in $(0, c)$ as a complete set of even ultraspherical Gegenbauer polynomials $C_{2m}^{1/6}(y/c)$. Thus the basis functions for $F^{s,a}(y)$ in this case are found to be

$$f_m^s(y) = f_m^a(y) = f_m(y) = -\frac{\mathrm{d}}{\mathrm{d}y}\left[\mathrm{e}^{-ky}\int_y^c \mathrm{e}^{Kt}\widehat{f}_m(t)\,\mathrm{d}t\right], \quad 0 < y < c \tag{A2.12}$$

where $\widehat{f}_m(y)$ is chosen as

$$\widehat{f}_m(y) = \frac{2^{7/6}\Gamma(1/6)(2m)!}{\pi\Gamma(2m+\frac{1}{3})c^{1/3}(c^2-y^2)^{1/3}}C_{2m}^{1/6}\left(\frac{y}{c}\right), \quad 0 < y < c. \tag{A2.13}$$

(iii) $y \in \overline{L}_3 = (0, a) + (c, h)$.

In this case we have to choose two sets of basis functions, $p_m^{s,a}(y)$ for $0 < y < a$ and $q_m^{s,a}(y)$ for $c < y < h$. The choice for $p_m^{s,a}(y)$ is the same as that given by the expression in the relation (A2.12) (along with (A2.13)) with c replaced by a, and similarly, $q_m^s(y)$ for $c < y < h$ is the same as the expression given in the relation (A2.5) with a replaced by c while $q_m^a(y)$ for $c < y < h$ is the same as the expression given in the relation (A2.6) with a replaced by c.

(iv) $y \in \overline{L}_4 = (a, c)$.

In this case we have to consider only the behaviour $F^{s,a}(y) \sim (y-a)^{-1/3}$ as $y \to a+0$ and $F^{s,a}(y) \sim (c-y)^{-1/3}$ as $y \to c-0$. Also $F^s(y)$ satisfies the additional requirement (see Equation (3.25))

$$\int_a^c F^s(y)\,\mathrm{d}y = 0. \tag{A2.14}$$

Noting again the result

$$\int_a^c \frac{1}{(\frac{c-a}{2})^{1/3}\{(y-a)(c-y)\}^{1/3}}C_n^{1/6}\left(\frac{2y-a-c}{c-a}\right)\mathrm{d}y$$

$$= \int_{-1}^1 (1-t^2)^{-1/3}C_n^{1/6}(t)\,\mathrm{d}t = 0 \quad \text{for } n > 0, \tag{A2.15}$$

we observe that the basis functions for $F^s(y)(a < y < c)$ are given by

$$f_m^s(y) = g_{m+1}^{(2)}(y), \quad m = 0, 1, 2, \ldots, \tag{A2.16}$$

while the basis functions for $F^a(y)(a < y < c)$ are given by

$$f_m^a(y) = g_m^{(2)}(y), \quad m = 0, 1, 2, \ldots, \tag{A2.17}$$

where

$$g_m^{(2)}(y) = \frac{2^{1/6}\Gamma(1/6)m!}{\pi\Gamma(m+1/3)(\frac{c-a}{2})^{1/3}\{(y-a)(c-y)\}^{1/3}} C_m^{1/6}\left(\frac{2y-a-c}{c-a}\right), \quad a < y < c. \tag{A2.18}$$

Appendix III. Expressions for $K_{mn}^{s,a}$, $d_m^{s,a}$ etc

(i) For $\overline{L} = \overline{L}_1 = (a, h)$, we find that

$$K_{mn}^s = \frac{\delta_0}{\cosh^2 k_0 h}\left[(-1)^{m+n}\sum_{r=1}^{\infty}\left\{\frac{4J_{2n+(13/6)}\{k_r(h-a)\}J_{2m+(13/6)}\{k_r(h-a)\}}{\delta_r\{k_r(h-a)\}^{1/3}} + \frac{2}{r\pi}\coth\frac{r\pi b}{h-a}\frac{J_{2n+(13/6)}(r\pi)J_{2m+(13/6)}(r\pi)}{(r\pi)^{1/3}}\right\}\right], \tag{A3.1}$$

where J's are Bessel functions of first kind, and

$$d_m^s = \frac{1}{\cosh k_0 h}\frac{I_{2m+(13/6)}\{k_0(h-a)\}}{\{k_0(h-a)\}^{1/6}}, \tag{A3.2}$$

where I's are modified Bessel functions of first kind. The expression for K_{mn}^a is obtained from $K_{m-1,n-1}^s$ with 'coth' replaced by 'tanh' and inserting an extra term $(12\pi b/h-a)/(2^{1/3}/\{\Gamma(1/3)\}^4)\,\delta_{0n}\delta_{0m}$ inside the square bracket, where $\delta_{0n} = 1$ for $n = 0$ and $\delta_{0n} = 0$ for $n \geqslant 1$. We also note that

$$d_m^a = d_{m-1}^s. \tag{A3.3}$$

(ii) For $\overline{L} = \overline{L}_2 = (0, c)$, we find that

$$K_{mn}^s = \frac{\delta_0}{\cosh^2 k_0 h}\left[4(-1)^{m+n}\sum_{r=1}^{\infty}\left\{\frac{\cos^2 k_r h}{\delta_r}\frac{J_{2n+(1/6)}(k_r c)J_{2m+(1/6)}(k_r c)}{(k_r c)^{1/3}} + \frac{\coth\alpha_r b\cos^2\alpha_r c}{\gamma_r}\frac{J_{2n+(1/6)}(\alpha_r c)J_{2m+(1/6)}(\alpha_r c)}{(\alpha_r c)^{1/3}}\right\} - \frac{\cot\alpha_0 b}{\gamma_0}\cosh\alpha_0 c\frac{J_{2n+(1/6)}(\alpha_0 c)I_{2m+(1/6)}(\alpha_0 c)}{(\alpha_0 c)^{1/3}}\right], \tag{A3.4}$$

$$d_{mn}^{s,a} = \frac{I_{2m+(1/6)}(k_0 c)}{(k_0 c)^{1/6}} \tag{A3.5}$$

and the expression for K_{mn}^{a} is obtained from K_{mn}^{s} in the relation (A3.4) by replacing 'coth' by 'tanh' and '$-$ cot' by 'tan'.

(iii) For $\overline{L} = \overline{L}_3 = (0, a) + (c, h)$, we find that G_{mn}^{s} is obained from K_{mn}^{s} in the relation (A3.4) by replacing c by a while Q_{mn}^{s} is obtained from K_{mn}^{s} in the relation (A3.1) by replacing a by c. Again, H_{mn}^{s} is given by

$$H_{mn}^{s} = \frac{4(-1)^{n+m+1}\delta_0}{\cosh^2 k_0 h} \sum_{r=1}^{\infty} \frac{\cos k_r h}{\delta_r} \frac{J_{2n+(13/6)}\{k_r(h-c)\} J_{2m+(13/6)}(k_r a)}{\{k_r(h-c)\}^{1/6}(k_r a)^{1/6}} \tag{A3.6}$$

and P_{mn}^{s} is given by

$$P_{mn}^{s} = H_{nm}^{s}. \tag{A3.7}$$

We obtain the expression for G_{mn}^{a} from K_{mn}^{s} in the relation (A3.4) by replacing c by a, 'coth' by 'tanh' and 'cot' by 'tan', while we have the relations:

$$H_{mn}^{a} = H_{m,n-1}^{s}, \tag{A3.8}$$

$$P_{mn}^{a} = P_{m-1,n}^{s}, \tag{A3.9}$$

$$Q_{mn}^{a} = Q_{m-1,n-1}^{s}, \tag{A3.10}$$

$$d_{m}^{(1)_s} = \frac{I_{2m+(1/6)}(k_0 a)}{(k_0 a)^{1/6}}, \tag{A3.11}$$

$$d_{m}^{(2)_s} = \frac{1}{\cosh k_0 h} \frac{I_{2m+(7/6)}\{k_0(h-c)\}}{\{k_0(h-c)\}^{1/6}}, \tag{A3.12}$$

$$d_{m}^{(1)_a} = d_{m}^{(1)_s}, \tag{A3.13}$$

$$d_{m}^{(2)_a} = d_{m-1}^{(2)_s}. \tag{A3.14}$$

(iv) $\overline{L} = \overline{L}_4 = (a, c)$.

$$\begin{aligned} K_{mn}^{s} = \frac{\delta_0}{\cosh^2 k_0 h} \Bigg[\sum_{r=1}^{\infty} \Bigg\{ & \frac{4}{\delta_r (k_r(\frac{c-a}{2})^{1/3}} \begin{pmatrix} (-1)^{n+1/2} \cos k_r(h - \frac{c+a}{2}) \\ (-1)^{n/2} \sin k_r(h - \frac{c+a}{2}) \end{pmatrix} \\ & \times \begin{pmatrix} (-1)^{m+1/2} \cos k_r(h - \frac{c+a}{2}) \\ (-1)^{m/2} \sin k_r(h - \frac{c+a}{2}) \end{pmatrix} \\ & \times J_{n+(7/6)}\left(k_r \frac{c-a}{2}\right) J_{m+(7/6)}\left(k_r \frac{c-a}{2}\right) \\ & + \left(\frac{2}{r\pi}\right)^{4/3} \coth \frac{r\pi b}{c-a} \begin{pmatrix} (-1)^{n+1/2} \cos \frac{r\pi}{2} \\ (-1)^{n/2} \sin \frac{r\pi}{2} \end{pmatrix} \\ & \times J_{n+(7/6)}\left(\frac{r\pi}{2}\right) J_{m+(7/6)}\left(\frac{r\pi}{2}\right) \Bigg\} \Bigg], \end{aligned} \tag{A3.15}$$

where the upper terms are for odd n, odd m while the lower ones are for even n, even m.

$$d_m^s = \frac{(-1)^{m+1}\, e^{k_0(h-(c+a/2))} + e^{-k_0(h-(c+a/2))}}{2\cosh k_0 h} \frac{I_{m+(7/6)}(k_0 \frac{c-a}{2})}{(k_0 \frac{c-a}{2})^{1/6}}. \tag{A3.16}$$

K_{mn}^a is obtained from $K_{m-1,n-1}^s$ with 'coth' replaced by 'tanh' and by insertion of the extra term $(12\pi b/c - a)(2^{1/3}/\{\Gamma(\frac{1}{3})\}^4)\delta_{0n}\delta_{0m}$ inside the square bracket. Finally,

$$d_m^a = d_{m-1}^s. \tag{A3.17}$$

Appendix IV. Effect of the introduction of a constant in the solution of $\phi^s(x, y)(0<x<b, y\in\overline{L}_j, j=1,3,4)$

We prove here that, in the present method of calculation of the reflection coefficient, the introduction of the constant term in the solution of $\phi^s(x, y)$ in the region $0 < x < b, y \in \overline{L_j}$ $(j = 1, 3, 4)$, does not have any effect. We consider the case $y \in \overline{L_1}$ only. The cases $y \in \overline{L_3}$ or $y \in \overline{L_4}$ can be dealt with similarly.

Let us include a constant B_0^s to the expression for $\phi^s(x, y)$ given in the relation (3.8), *i.e.* $\phi^s(x, y)$ is now expressed as

$$\phi^s(x, y) = B_0^s + \sum_{n=1}^{\infty} B_n^s \cosh\frac{n\pi x}{h-a} \cos\frac{n\pi(y-a)}{h-a}, \quad 0 < x < b, a < y < h, \tag{A4.1}$$

where $B_n^s (n \geqslant 1)$ is given by the relation (3.20).

To find B_0^s, we use the *integral law of action and reaction* (*cf.* Driemer *et al.* [33]) to the section $a < y < h$ at $x = b$, so that

$$\int_a^h \phi^s(b-0)\,dy = \int_a^h \phi^s(b+0)\,dy. \tag{A4.2}$$

In the Equation (A4.2), we evaluate the left side by using the expression of $\phi^s(x, y)$ given in (A4.1) and the right side by using the expression of $\phi^s(x, y)$ given in Equation (3.6). Thus, we find that

$$B_0^s = \frac{1}{h-a}\left[\frac{1+R^s}{\cosh k_0 h}\frac{\sinh k_0(h-a)}{k_0} + \sum_{n=1}^{\infty} A_n^s \frac{\sin k_n(h-a)}{k_n}\right], \tag{A4.3}$$

where $A_n^s (n \geqslant 1)$ is given in the relation (3.17).

Again, we find that $\mathcal{M}^s(y, u)$ for this case is changed to $\mathcal{M}_0^s(y, u)$ where $\mathcal{M}_0^s(y, u)$ is given by

$$\mathcal{M}_0^s(y, u) = \mathcal{M}^s(y, u) - \frac{\delta_0}{\cosh^2 k_0 h} \sum_{r=1}^{\infty} \frac{\cos k_r(h-u)}{\delta_r} \frac{\sin k_r(h-a)}{k_r(h-a)}. \tag{A4.4}$$

In Equation (A4.4), the expression for $\mathcal{M}^s(y, u)$ is given by Equation (A1.1), and the second term arises due to the introduction of B_0^s in $\phi^s(x, y)$. We note that this second term does not involve the variable y.

Thus, Equation (3.27) for this case is changed to

$$\int_a^h F^s(u)\mathcal{M}_0^s(y,u)\,\mathrm{d}u = \frac{1}{\cosh k_0 h}\left[\cosh k_0(h-y) - \frac{\sinh k_0(h-a)}{k_0(h-a)}\right], \tag{A4.5}$$

where the second term in the right side arises due to the presence of B_0^s in $\phi^s(x, y)$.

The Equation (3.35) for this case is changed to

$$\sum_{n=0}^{N} a_n^s L_{mn}^s = D_m^s, \quad m = 0, 1, 2, \ldots, N \tag{A4.6}$$

where

$$\begin{aligned} L_{mn}^s &= \int_a^h \int_a^h \mathcal{M}_0^s(y,u) f_n^s(u) f_m^s(y)\,\mathrm{d}u\,\mathrm{d}y \\ &= K_{mn}^s - \frac{\delta_0}{\cosh k_0 h}\sum_{r=1}^{\infty} \frac{\sin k_r(h-a)}{\delta_r k_r(h-a)} \int_a^h \cos k_r(h-u) f_n^s(u)\,\mathrm{d}u \int_a^h f_m^s(y)\,\mathrm{d}y, \end{aligned} \tag{A4.7}$$

and

$$D_m^s = d_m^s - \frac{\sinh k_0(h-a)}{k_0(h-a)\cosh k_0 h}\int_a^h f_m^s(y)\,\mathrm{d}y, \tag{A4.8}$$

K_{mn}^s being given by Equation (A3.1) and d_m^s being given by Equation (A3.2). By using Equations (A2.5), (A2.6) and (A2.4), we find that

$$\int_a^h f_m^s(y)\,\mathrm{d}y = \int_a^h g_{m+1}^{(1)}(y)\,\mathrm{d}y = 0, \quad m = 0, 1, 2, \ldots, N. \tag{A4.9}$$

Using the result (A4.9) in Equation (A4.7) and (A4.8), we find that

$$L_{mn}^s = K_{mn}^s \quad \text{and} \quad D_{mn}^s = d_{mn}^s,$$

so that Equation (A4.6) reduces to Equation (3.35). Thus, the introduction of a constant in the solution of ϕ^s for the case of type I barrier does not affect the final results.

We have also checked that for type III and IV barriers, the introduction of a constant does not affect Equation (3.35). Thus, the introduction of a constant term in the solution of $\phi^s(x, y)$ in the region $0 < x < b$, $y \in \overline{L_j}$ $(j = 1, 3, 4)$, does not affect the calculation of the reflection coefficient by the present method, but it may affect the calculation of other hydrodynamic quantities associated with the problem. This, however, has not been demonstrated here.

References

1. F. Ursell, The effect of a fixed vertical barrier on surface waves in deep water. *Proc. Camb. Phil. Soc.* 43 (1947) 374–382.
2. H. Levine and E. Rodemich, Scattering of surface waves on an ideal fluid. *Math. and Stat. Lab. Tech. Rep.* 78, Stanford University (1958) 1–64.
3. M. Lewin, The effect of vertical barriers on progressive waves. *J. Math. Phys.* 42 (1963) 287–300.
4. C. C. Mei, Radiation and scattering of transient gravity waves by vertical plates. *Q. J. Mech. Appl. Maths.* 19 (1966) 417–440.
5. W. E. Williams, Note on the scattering of water waves by a vertical barrier. *Proc. Camb. Phil. Soc.* 62 (1966) 507–509.
6. D. V. Evans, Diffraction of surface waves by a submerged vertical plate. *J. Fluid Mech.* 40 (1970) 433–451.

7. D. Porter, The transmission of surface waves through a gap in a vertical barrier. *Proc. Camb. Phil. Soc.* 71 (1972) 411–421.
8. Sudeshna Banerjea, Scattering of water waves by a vertical wall with gaps. *J. Austral. Math. Soc., Ser. B* 37 (1996) 512–529.
9. R. Porter and D. V. Evans, Complementary approximations to wave scattering by vertical barriers. *J. Fluid Mech.* 294 (1995) 155–180.
10. D. V. Evans and C. A. N. Morris, The effect of a fixed vertical barrier on obliquely incident surface waves in deep water. *J. Inst. Maths. Applics.* 9 (1972), 198–204.
11. B. N. Mandal and Pulak Das, Oblique diffraction of surface waves by a submerged vertical plate. *J. Engng. Math.* 30 (1996) 459–470.
12. Pulak Das, Sudeshna Banerjea and B. N. Mandal, Scattering of oblique waves by a thin vertical wall with a submerged gap. *Arch. Mech.* 48 (1996) 959–972.
13. I. J. Losada, M. A. Losada and A. J. Roldán, Propagation of oblique incident waves past rigid vertical thin barriers. *Appl. Ocean Res.* 14 (1992) 191–199.
14. B. N. Mandal and D. P. Dolai, Oblique water wave diffraction by thin vertical barriers in water of uniform finite depth. *Appl. Ocean Res.* 16 (1994) 195–203.
15. D. V. Evans and C. A. N. Morris, Complementary approximations of the solution of a problem in water waves. *J. Inst. Maths. Applics.* 10 (1972) 1–9.
16. Mridula Kanoria and B. N. Mandal, Oblique wave diffraction by two parallel vertical barriers with submerged gaps in water of uniform finite depth. *J. Tech. Phys.* 37 (1996) 187–204.
17. Sudeshna Banerjea, Mridula Kanoria, D. P. Doali and B. N. Mandal, Oblique wave scattering by a submerged thin wall with gap in finite depth water. *Applied Ocean Research* 18 (1996) 319–327.
18. Pulak Das, D. P. Dolai and B. N. Mandal, Oblique water wave diffraction by two parallel thin barriers with gaps. *J. Wtry. Port Coast Ocean Engng.* 123 Aug (1997) 163–171.
19. E. O. Tuck, Transmission of water waves through small apertures. *J. Fluid Mech.* 49 (1971) 481–491.
20. E. O. Tuck, Matching problems involving flow through small holes. *Adv. Fluid Mech.* 15 (1975) 89–158.
21. B. A. Packham and W. E. Williams, A note on the transmission of water waves through small apertures. *J. Inst. Maths Applics.* 10 (1972) 176–184.
22. B. N. Mandal, A note on the diffraction of water waves by a vertical wall with a narrow gap. *Arch. Mech.* 39 (1987) 269–273.
23. T. H. Havelock, Forced surface waves on water. *Phil. Mag.* 8 (1929) 569–576.
24. D. C. Guiney, B. J. Noye and E. O. Tuck, Transmission of water waves through small apertures. *J. Fluid Mech.* 55 (1972) 149–161.
25. D. Owen and B. S. Bhatt, Transmission of water waves through a small aperture in a vertical thick barrier. *Q. J. Mech. Appl. Math.* 38 (1985) 379–409.
26. P. L.-F. Liu and J. Wu, Transmission of oblique waves through submerged apertures. *Appl. Ocean. Res.* 8 (1986) 144–150.
27. P. L.-F. Liu and J. Wu, Wave transmission through submerged apertures. *J. Wtry. Port Coast and Ocean Engng. ASCE* 113 (1987) 660–671.
28. C. C. Mei and J. L. Black, Scattering of surface waves by rectangular obstacles in waters of finite depth. *J. Fluid Mech.* 38 (1969) 499–511.
29. D. V. Evans and M. Fernyhough, Edge waves along periodic coastlines, Part 2. *J. Fluid Mech.* 297 (1995) 307–325.
30. J. N. Newman, Propagation of water waves past long two-dimensional obstacles. *J. Fluid Mech.* 23 (1965) 23–29.
31. P. A. Martin and R. A. Dalrymple, Scattering of long waves by cylindrical obstacles and gratings using matched asymptotic expansions. *J. Fluid Mech.* 188 (1988) 465–490.
32. P. McIver, Low-frequency asymptotics of hydrodynamic forces on fixed and floating structures. In M. Rahman (ed.), *Ocean Wave Engineering*. Southampton: Computational Mechanics Publications, U.K. (1994) 1–49.
33. N. Drimmer, Y. Agnon and M. Steassnie, A simplified analytical model for a floating breakwater in water of finite depth. *Appl. Ocean Res.* 14 (1992) 33–41.